Homeodomain protein Sxi1α regulates cell-cell fusion during distinct sexual reproduction modes in *Cryptococcus deneoformans*

Jun Huang, Patricia P. Peterson, Ziyan Xu, Liping Xiong, Sheng Sun, and Joseph Heitman*

Department of Molecular Genetics and Microbiology, Duke University Medical Center, Durham, NC 27710, USA

* Corresponding author: Joseph Heitman
Email: heitm001@duke.edu
Keywords: Homeodomain protein; Cell-cell fusion; Unisexual reproduction.

Abstract

Sex-specific homeodomain (*HD*) proteins are key regulators of cell identity and sexual development in fungi, typically functioning as heterodimers to regulate transcription. In the human fungal pathogens *Cryptococcus neoformans* and *Cryptococcus deneoformans*, the *HD* proteins Sxi1α and Sxi2**a** (sex-induced 1α and 2**a**) have been characterized as interacting partners that play critical roles in sexual development during **a** x α sexual reproduction. Given the dominance of α cells in natural populations of *Cryptococcus*, the roles of Sxi1α and Sxi2**a** in unisexual reproduction, which predominantly involves same-sex (α x α) mating, remain unclear. To elucidate the functions of Sxi1α and Sxi2**a** in unisexual reproduction, we first used AlphaFold3 to predict their structures, which revealed the potential for both heterodimeric and homodimeric complexes. We subsequently deleted *SXI1*α and *SXI2***a** in the hyperfilamentous self-fertile *C. deneoformans* strains XL280**a** and XL280α. Disruption of these genes did not result in noticeable defects in vegetative growth, virulence-associated traits, colony morphology, sporulation, or competitiveness during either **a** x α or α x α crosses. Surprisingly, the absence of *SXI1*α significantly increased the cell–cell fusion rate during both α x α and **a** x α mating, suggesting a novel inhibitory role for Sxi1α, independent of the partner Sxi2**a**. Together, our findings revealed an unexpected function of Sxi1α in regulating cell fusion, which may contribute to the predominance of *MAT*α isolates in global *Cryptococcus* populations and the conservation of *SXI1*α in a population that is predominantly α mating type.

45 **Introduction**

46 Sexual reproduction is a key process in eukaryotic organisms, promoting genetic diversity and
47 facilitating adaptation under changing environments. In fungi, this process is controlled by the mating-type
48 (*MAT*) locus, a specific genomic region containing genes required for successful mating. Among these
49 genes, pheromone and pheromone receptors (*P/R*) are involved in signal transduction and recognition
50 between mating partners, and homeodomain (*HD*) transcription factors act as master regulators that
51 control the expression of genes necessary for sexual development (Yadav et al. 2023). In the model yeast
52 *Saccharomyces cerevisiae*, Mat**a**1 and Matα2 are well-characterized HD proteins, forming heterodimers
53 that bind DNA cooperatively to repress transcription of cell type-specific genes (Goutte and Johnson
54 1988; Li et al. 1995). Unlike *MAT***a**1,which promotes **a**-specific gene expression, *MAT*α2 can form
55 homodimers to repress **a**-specific genes (Keleher et al. 1988; Herskowitz 1989; Goutte and Johnson
56 1993). In the corn smut fungus *Ustilago maydis*, HD proteins bWest (bW) and bEast (bE) dimerize to
57 regulate fungal morphological switching, and interactions with the plant hosts (Gillissen et al. 1992;
58 Kämper et al. 1995; Wahl et al. 2010; Vollmeister et al. 2012). Similarly, sexual development in the
59 mushroom *Coprinus cinereus* requires the physical interaction of two HD proteins, HD1 and HD2 (Kües et
60 al. 1994).

61 In the human fungal pathogens *Cryptococcus neoformans* (formerly *C. neoformans* var. *grubii*,
62 serotype A) and its sister species *C. deneoformans* (formerly *C. neoformans* var. *neoformans,* serotype
63 D*)*, the *P/R* and *HD* genes as well as additional genes reside in a relatively large (>100 kb) *MAT* locus
64 (Hull et al. 2005; Sun, Coelho, et al. 2019; Bian et al. 2024). In addition to its role sexual reproduction, the
65 *MAT* locus has been associated with several non-mating functions in *Cryptococcus*, including fungal
66 virulence and uniparental mitochondrial inheritance (mito-UPI), in which mitochondrial DNA is
67 predominantly inherited from the *MAT***a** parent after a x α sexual reproduction. (Kwon-Chung and Bennett
68 1978; Yan et al. 2004). We previously identified the *Cryptococcus* sex-specific HD proteins Sxi1α (Sex
69 inducer 1α) and Sxi2**a** (Sex inducer 2**a**), which heterodimerize and are involved in cell identify, sexual
70 development, and mito-UPI during **a** x α bisexual reproduction, with evidence indicating that, beyond
71 Sxi1α and Sxi2**a** , the *P/R* locus is involved in mito-UPI process as well. (Hull et al. 2002; Hull et al. 2004;
72 Yan et al. 2004; Yan et al. 2004; Hull et al. 2005; Sun et al. 2020). Several conserve and novel

73 downstream targets (e.g., *CLP1* (clampless 1) and *CPR2* (*Cryptococcus* pheromone receptor 2)) of Sxi1α
74 and Sxi2**a** involved in sexual reproduction have been identified (Ekena et al. 2008; Hsueh et al. 2009;
75 Heimel et al. 2010; Mead et al. 2015). Additional evidence suggests that Sxi1α is not required for
76 virulence in *C. neoformans* (Hull et al. 2004) and the role of Sxi2**a** in virulence remains unclear. In
77 addition to **a** x α bisexual reproduction, unisexual reproduction can also occur between partners of the
78 same mating type (mainly α x α) in *C. neoformans* and *C. deneoformans* (Lin et al. 2005). In natural
79 *Cryptococcus* populations, *MAT*α isolates are predominant among both clinical and environmental
80 samples, suggesting that **a** x α heterothallic sexual reproduction is infrequent (Kwon-Chung and Bennett
81 1978; Desjardins et al. 2017). This strong bias in *MAT* locus distribution may, at least in part, be explained
82 by the occurrence of unisexual reproduction, which enables genetic recombination and propagation in the
83 absence of a compatible mating partner (Lin et al. 2005; Sun et al. 2014; Roth et al. 2018). As key sex-
84 specific transcriptional regulators, the roles of Sxi1α and Sxi2**a** in unisexual reproduction remain to be
85 elucidated.

86 In this study, we sought to determine whether Sxi1α and Sxi2**a** are involved in same-sex mating
87 in *Cryptococcus*. Protein prediction via AlphaFold3 suggested that Sxi1α and Sxi2**a** can dimerize and
88 potentially form both heterodimer as well as homodimers. Taking advantage of the hyperfilamentous *C.*
89 *deneoformans* congenic isolates XL280α and XL280**a**, along with the CRISPR/Cas9 gene editing system,
90 we deleted *SXI1*α and *SXI2***a** in XL280α and XL280**a**, respectively. Consistent with previous results, we
91 found that *SXI1*α and *SXI2***a** are dispensable for vegetative growth and multiple virulence factors,
92 including thermotolerance at 37°C, polysaccharide capsule formation, and melanin production.
93 Interestingly, no obvious defects in colony morphology, hyphal development, basidium formation,
94 sporulation, spore germination or competitiveness were detected in *sxi1*αΔ or *sxi2***a**Δ mutants during
95 unisexual reproduction. In contrast, we found that Sxi1αΔ with significantly increased cell-cell fusion
96 frequency during both α x α and **a** x α crosses. Overall, our results suggest a novel function of Sxi1α in
97 regulating cell-cell fusion, which may influence the sexual reproduction in global populations of
98 *Cryptococcus*.

99

100 **Materials and methods**

101 **Fungal strains and growth conditions**

102 *C. deneoformans* and *C. neoformans* strains for this study are listed in Table S1. The strains were
103 stored in 15% glycerol at -80°C for long-term storage. Fresh strains were streaked from glycerol stock
104 and maintained on solid YPD medium (1% yeast extract, 2% Bacto Peptone, 2% dextrose) at 30°C.

105 Spot dilution assays were performed with overnight cultures of the tested strains grown in liquid
106 YPD at 30°C. Strains were diluted to an OD_{600} of 0.5 in sterile water. These cultures were further serially
107 diluted 5-fold and spotted (3 μL for each dilution) onto YPD plates. The plates were incubated at 30°C and
108 37°C (testing thermotolerance) for 2 days before imaging.

109

110 **Protein structural predictions**

111 Protein structure predictions were made with AlphaFold3 (Abramson et al. 2024) on the
112 AlphaFold server (https://alphafoldserver.com/). The predicted models and error plots were further
113 processed with Chimera X (v 1.9) (Meng et al. 2023) for predicted local distance difference test (pLDDT)
114 value filtering, alignment, and visualization.

115

116 **Gene deletion and confirmation**

117 Approximately 1.0 kb 5' and 3' flanking regions of *SXI1*α and 60 bp 5' and 3' flanking regions of
118 *SXI2***a** were constructed using primers listed in Table S2 to target their respective genes for homologous
119 recombination. Overlap PCR with a selectable marker was used to construct the DNA donor with 1.0 kb
120 homology, while 60 bp microhomology was included in the primers for donor amplification. *C. neoformans*
121 codon optimized Cas9, gRNAs (a single gRNA targeting *SXI1*α and two gRNAs targeting *SXI2***a**), and
122 drug resistance cassettes (*NAT* from pAI3 or *NEO* from pJAF1) containing homologous flanking
123 sequences were introduced into XL280 wild-type strains via the previously reported Transient CRISPR-
124 Cas9 Coupled with Electroporation (TRACE) system (Fan and Lin 2018; M.Y. Huang et al. 2022).
125 Transformants were screened using internal PCR to the ORF, and 5′ and 3′ junction PCR to the drug
126 resistance maker to confirm integration at the genomic locus. Illumina whole-genome sequencing was
127 performed on positive transformants using Novaseq X Plus platform (2x150 bp). The sequencing reads

128 were mapped to a modified version of the XL280α genome (Fu et al. 2021) with Burrows-Wheeler
129 Alignment tool (BWA) (v 0.7.17) (Li and Durbin 2009) to further confirm the deletion mutant strains. The
130 modification included adding the *MAT***a** locus sequence of JEC20 (GenBank: AF542530.2) as an
131 additional contig.
132
133 **Capsule formation and melanin production assays**
134 Tested strains, with an initial OD_{600} of 0.1 in 4 mL liquid RPMI medium (RPMI 1640 with 2%
135 dextrose), were incubated on a roller drum at 70 rpm and 30°C for 3 days. After washing and
136 resuspension in water, the cells were negatively stained with an equal volume of India ink to visualize the
137 capsules.
138 To assess melanin production, overnight saturated cultures of test strains were spotted (10 μL)
139 onto Niger seed agar plates (7% Niger seed, 0.1% dextrose). The Niger seed plates were incubated at
140 30°C and 37°C for 8 days before photographing.
141
142 **Competition assays**
143 Overnight cultures of tested strains grown in liquid YPD at 30°C were diluted to OD_{600} of 0.2 and
144 equally mixed in a 1:1 ratio in 5 mL of liquid YPD for co-culture. *sxi1*αΔ::*NAT* mutants (resistant to NAT)
145 and *sxi2***a**Δ::*NEO* mutants (resistant to G418) were mixed with XL280α and XL280**a**, respectively. The
146 mixture was plated on YPD plates, YPD + nourseothricin (NAT), and YPD + neomycin (G418) to confirm
147 starting ratio. After 24 and 48 hours of co-culture, an aliquot of the mixture was sampled and plating was
148 repeated with OD_{600} diluted to 0.1 to track changes in relative abundance of mutants. Four independent
149 replicates were performed for each competition.
150 For the competition assay performed on MS medium, overnight cultures were similarly diluted to
151 OD_{600} of 1. *sxi1*αΔ::*NAT* or *sxi2***a**Δ::*NEO* mutants and the corresponding XL280 wildtype strain were
152 equally mixed in a 1:1 ratio and spotted on MS medium. Spores were dissected 10 to 14 days post
153 spotting. Yeast cells from internal regions were also collected. Spores or yeast cells were further
154 transferred to YPD+NAT, YPD+G418 and YPD to determine the ratio of mutants in the population. Five
155 independent spots were investigated for each competition.

156 **Mating and cell-cell fusion assay**

157 Mating plates were set up as described previously (Sun, Priest, et al. 2019). α x α unisexual and
158 **a** x α sexual reproduction assays were performed on Murashige and Skoog (MS, Sigma, USA) plates for
159 1 to 2 weeks before imaging and dissection. Basidiospores generated during unisexual reproduction were
160 randomly dissected and plated on YPD plates for 2 to 3 days to determine spore viability and germination
161 rates.

162 Cell-cell fusion frequency during α x α unisexual outcrossing in XL280α *NAT* (XL561 and XL562)
163 and XL280α *NEO* (XL563 and XL564) was compared to bilateral mutant crosses of *sxi1*αΔ::*NAT* and
164 *sxi1*αΔ: *NEO* or the unilateral crosses of *sxi1*αΔ::*NAT* and XL280α *NEO*. Additionally, XL280α *NAT*
165 (XL561) and XL280**a** *NEO* (JHG223) were used as wildtype strains to test the role of *SXI1*α and *SXI2***a** in
166 cell-cell fusion during **a** x α sexual reproduction. Both bilateral (*sxi1*αΔ::*NAT* x *sxi2***a**Δ::*NEO*) and unilateral
167 crosses (*sxi1*αΔ::*NAT* x XL280**a** *NEO* and XL280α *NAT* x *sxi2***a**Δ::*NEO*) were analyzed.

168 Cells were diluted in sterile water to an OD_{600} of 1. Two *MAT*α strains (α x α outcrossing)
169 containing either *NAT* or *NEO* resistance cassettes were mixed equally with JEC20 (*MAT***a**) for assisted
170 mating on V8 agar (pH = 7.0) and incubated for 72 hours in the dark at room temperature. For **a** x α
171 crossing, cells were prepared similarly but without adding additional JEC20 on V8 agar (pH = 7.0) and
172 incubated for 48 hours in the dark at room temperature. The cells were then collected and plated on YPD
173 + NAT + G418 and YPD alone to determine the ratio of colonies with dual resistance 4 to 5 days post-
174 plating (i.e., fusion product) out of the total cells. It should be noted that when screening for fusion
175 products from crosses between XL280**a** *NEO* and XL280α *NAT* on YPD+NAT+G418 rich medium plates,
176 we observed that in addition to colonies formed by yeast cells, there were also tiny colonies that produced
177 extensive hyphae with occasional formation of basidia and basidiospore chains. It is not yet clear what is
178 the nature of these highly filamentous colonies, and thus, in the current analysis we only included yeast-
179 like colonies for clarity.

180

181 **Light and scanning electron microscopy (SEM)**

182 Mating structures from MS plates were imaged with an AxioSkop 2 fluorescence microscope to
183 visualize hyphae, basidia and basidiospores under brightfield. SEM samples were prepared following a

184 previously described protocol (Peterson et al., 2024), with minor modifications. Briefly, a ~2 cm × 2 cm
185 agar plug containing patch of mated cells from MS plates was fixed in PBS containing 4% formaldehyde
186 and 2% glutaraldehyde at 4°C for 2 hours. The fixed samples were then gradually dehydrated in a graded
187 ethanol series (30%, 50%, 70%, 95%), with each step performed at 4°C for 15 min. This was followed by
188 three washes in 100% ethanol, each at 4°C for 15 min. The samples were further dehydrated using a
189 Ladd CPD3 Critical Point Dryer and subsequently coated with a thin layer of gold with a Denton Desk V
190 Sputter Coater (Denton Vacuum, USA). Hyphae, basidia and basidiospores were observed with a
191 scanning electron microscope equipped with an EDS detector (Apreo S, ThermoFisher, USA).
192
193 **Statistical analysis**
194 Paired or unpaired student t-tests were performed in Rstudio (version 2024.04.1+748) using the “t.test”
195 function with argument “paired = TRUE” for paired tests or “paired = FALSE” for unpaired tests.

196 **Results and Discussion**

197 **Sxi1α and Sxi2a are predicted to form a heterodimer**

198 To study the impacts of the homeodomain proteins Sxi1α and Sxi2**a** on unisexual reproduction in
199 *Cryptococcus*, we selected to study XL280α and XL280**a**, a pair of congenic strains of *C. deneoformans*,
200 that are well-known for the ability to undergo unisexual reproduction which exhibit robust self-
201 filamentation and sporulation (Lin et al. 2005; Zhai et al. 2013). Sxi1α and Sxi2**a** are conserved between
202 *C. neoformans* and *C. deneoformans*, and homeodomain (Pfam:00046) or homeobox KN domains (from
203 **KN**OX family transcription factors, Pfam:PF05920) were found within the sequences via NCBI conserved
204 domain search (Figure 1A). Both domains are structurally related, sharing DNA-binding functions through
205 a helix-turn-helix motif, suggesting potential functional relevance in regulating gene expression. Similar to
206 our previous report with yeast two-hybrid analysis (Hull et al. 2002; Hull et al. 2005), a heterodimer
207 between Sxi1α and Sxi2**a** was predicted by AlphaFold3 protein-protein complex prediction (Figure 1B).
208 Pairwise structural alignments between the predicted Sxi1α-Sxi2**a** heterodimer and the crystal structure of
209 the *S. cerevisiae* MAT**a**1-MATα2 heterodimer (Li 1998) revealed robust structural similarity between the
210 two homeodomain complexes with an RMSD value of 0.561 angstroms between 49 pruned atom pairs
211 (Figure 1C). Similarly, the Sxi1α-Sxi2**a** heterodimer exhibited high structural similarity to the AlphaFold3-
212 predicted bW-bE heterodimer from the corn smut fungus *Ustilago maydis*, with a RMSD of 1.069
213 angstroms across 40 pruned atom pairs, supporting a conserved structure for the *MAT* locus-specific HD
214 complex in fungi.

215 Previous studies showed that, in addition to forming a heterodimer with MAT**a**1, *S. cerevisiae*
216 MATα2 forms a homodimer to repress **a**-specific genes (Dranginis 1990). Therefore, we tested whether
217 Sxi1α and Sxi2**a** can also form homodimers. AlaphaFold3 predicted the potential formation of a low-
218 confidence homodimer of Sxi1α-Sxi1α (ipTM = 0.14 pTM = 0.23) and of Sxi2**a**-Sxi2**a** (ipTM = 0.2 pTM =
219 0.24) (Figure 1D). These predictions suggest weak interactions, and further experimental validation is
220 required to confirm if these may have biological relevance.

221

222

223

224 **Sxi1α and Sxi2a are dispensable for *in vitro* growth and virulence traits**

225 To further characterize the phenotypic impacts of Sxi1α and Sxi2**a**, we deleted *SXI1*α and *SXI2***a**
226 genes in XL280α and XL280**a**, respectively, with a CRISPR/Cas9-based strategy. In combination with a
227 previously established TRACE electroporation protocol (Fan and Lin 2018; M.Y. Huang et al. 2022),
228 several drug-resistant transformants (4 for XL280α *sxi1*αΔ::*NAT* and 2 for XL280**a** *sxi2***a**Δ::*NEO*) were
229 confirmed with correct genotypes as deletion mutants based on 5' junction, 3' junction, and ORF specific
230 PCR analysis (Figure 2A). Mapping of reads generated from Illumina whole-genome sequencing further
231 confirmed the complete deletion of the genes in all four *sxi1*αΔ mutants and one of the two *sxi2***a**Δ
232 mutants, and a partial gene deletion in the other *sxi2***a**Δ mutant. (Figure 2B). Interestingly, in some of the
233 mutants elevated read-depth were observed in the flanking regions used for homologous recombination
234 during gene deletion, indicating a potential concatemeric or ectopic insertion (J. Huang et al. 2022) of the
235 resistance cassette (Figure 2B).

236 We next performed competition assays to assess the impact of Sxi1α and Sxi2**a** on fungal fitness
237 during vegetative growth. Equal amounts of mutant and wildtype cells were mixed in liquid YPD and
238 incubated at 30°C to assess the population dynamics. All of the tested *sxi1*αΔ and *sxi2***a**Δ deletion strains
239 showed similar fitness compared to their respective wildtype strains after 24h or 48h of incubation
240 compared to the initial starting proportion (0h), and thus the mutations confer no fitness defect (Figure
241 2C). Additionally, we characterized the contributions of Sxi1α and Sxi2**a** to several major virulence traits:
242 thermotolerance at 37°C, capsule formation, and melanin production. Consistent with our previous reports
243 in *C. neoformans* (Hull et al. 2004), none of the *sxi1*αΔ or *sxi2***a**Δ deletion strains displayed altered
244 virulence traits compared to the XL280 wildtype strains (Figure 2, D-F). Taken together, these results
245 indicate that the loss of *SXI1*α and *SXI2***a** does not affect the fitness of the XL280 strain during vegetative
246 growth and has no impact on virulence-related traits.

247

248 **Sxi1α and Sxi2a are dispensable for morphology, sporulation and cell viability during unisexual**
249 **reproduction**

250 We next investigated whether Sxi1α and Sxi2**a** are involved in unisexual reproduction in the
251 XL280 background. When grown on mating and selfing inducing MS solid medium (Xue et al. 2007) as

252 solo-cultures, all of the tested *sxi1*αΔ and *sxi2***a**Δ mutants were able to produce elongated hyphae as well
253 as basidia and basidiospore chains at levels similar to their of XL280 wildtype controls (Figure 3, A-B),
254 with no discernable differences of basidium and basidiospores observed by scanning electron microscope
255 (SEM) (Figure 3C). Thus, the deletion of *SXI1*α and *SXI2***a** did not affect unisexual reproduction
256 morphologically. Additionally, we collected random meiotic basidiospores by microdissection to test the
257 effect of Sxi1α and Sxi2**a** on spore germination rates and cell viability and found no significant difference
258 in germination rates between spores produced by the *sxi1*αΔ mutants and XL280α (p-values: 0.6477 (Δ#4
259 vs XL280α) and 0.1788 (Δ#5 vs XL280α), unpaired t-test), as well as between spores produced by the
260 *sxi2***a**Δ mutants and XL280**a** (p-values 0.59 (Δ#6 vs XL280**a**:) and 0.7498 (Δ#7 vs XL280**a**), unpaired t-
261 test) (Figure 3D).
262 We previously observed that strains capable of undergoing unisexual reproduction exhibit higher
263 competitiveness than mutants with unisexual reproduction defects, attributing to enhanced hyphal growth
264 and sporulation (Phadke et al. 2013). To this end, for each deletion strain we mixed equal numbers of
265 cells from the mutant (containing dominant drug-resistant marker) and its wildtype control strain (sensitive
266 to drug), and spotted the mixture on MS medium to induce unisexual reproduction. After robust
267 sporulation was observed, we dissected two populations: 1) random basidiospores from the periphery
268 where sporulation occurs, and 2) the center of the spot where cells remain mostly as yeast (Figure 3E, left
269 panel). After the germination of the dissected spores/yeast cells, we transferred them onto YPD plates
270 containing selective drug (i.e., NAT or G418) to determine from which strain in the mixture did they
271 originate from. We found that for both Sxi1α and Sxi2**a**, the ratios between mutant and wildtype among
272 the basidiospores at the periphery were similar to those among the yeast cells at the center
273 (spores/yeast, p-values: 0.5398275 (*sxi1*αΔ) and 0.379667 (*sxi2***a**Δ), paired t-test), indicating the loss of
274 Sxi1α and Sxi2**a** did not affect fungal competitiveness during unisexual reproduction (Figure 3E, right
275 panel).
276
277 **Sxi1α is critical for cell-cell fusion**
278 In the presence of a helper strain serving as a pheromone donor, α x α outcrossing can be
279 facilitated in *C. deneoformans* in so called Ménage à trois matings (Hull et al. 2002; Lin et al. 2005).

280 Previously, our results from **a** x α sexual reproduction suggested that Sxi1α and Sxi2a function after cell-
281 cell fusion (Hull et al. 2005). Although cell-cell fusion is dispensable for unisexual reproduction, it may still
282 occur under certain conditions, such as during α x α outcrossing (Hull et al. 2002; Lin et al. 2005). Given
283 the limited understanding of Sxi1α's role in this context, we sought to determine whether Sxi1α is involved
284 in cell-cell fusion during α-α outcrossing. In the presence of a helper strain (JEC20, *MAT***a** *NAT*^{S} *NEO*^{S}),
285 equal numbers of cells from strains XL280α and *sxi1*αΔ that were differentially resistant to *NAT* and *NEO*
286 were mixed (*SXI1*α x *SXI1*αΔ, *SXI1*α x *sxi1*αΔ, and *sxi1*αΔ x *sxi1*αΔ) and spotted on V8 agar (pH=7.0) to
287 induce sexual reproduction. After 72 hours of incubation, cells were collected. We found fusion frequency
288 fewer than 5.04x10^{-8} in two independent of the XL280α *NAT* x XL280α *NEO* crosses, identified by
289 screening colonies for double resistance to NAT and G418. In contrast, significantly higher fusion
290 frequencies were found in *sxi1*αΔ::*NAT* x *sxi1*αΔ::*NEO* (22-fold higher than wildtype, frequency: 1.13x10^{-6},
291 p-value:0.00, unpaired t-test) and *sxi1*αΔ::*NAT* x XL280α *NEO* (62-fold higher than wildtype, frequency:
292 3.17x10^{-6}, p-value: 0.0080, unpaired t-test) (Figure 3F). Taken together, our results demonstrated that
293 cell-cell fusion between *MAT*α cells significantly increased when the *SXI1*α gene was absent in at least
294 one of the two strains.

295 We then asked whether Sxi1α, and possibly Sxi2**a** as well, have similar effects on cell-cell fusion
296 during **a** **x** α bisexual mating. Surprisingly, we found that *sxi1*αΔ x wildtype unilateral (2.3-fold higher than
297 wildtype, frequency:9.47x10^{-5}) and *sxi1*αΔ x *sxi2***a**Δ bilateral crosses (5.7-fold higher than wildtype,
298 frequency: 2.31x10^{-4}) exhibited significantly higher **a** x α cell fusion frequency than XL280 wildtype
299 crosses (frequency:4.04x10^{-5}) (p-value: 0.0273 (vs unilateral cross) and 0.0259 (vs bilateral cross) of
300 unpaired t-test) (Figure 3G). Interestingly, the fusion frequency of *sxi2***a**Δ unilateral crosses was similar to
301 the wildtype crosses (frequency:3.12x10^{-5}) (p-value: 0.2613 of unpaired t-test) (Figure 3G).

302 Previously, we found that the **a** x α cell fusion frequency in bilateral or unilateral crosses of *sxi1*αΔ
303 and *sxi2***a**Δ deletion strains in the auxotrophic background of *C. deneoformans* was 1.5- to 1.9-fold higher
304 than that of wildtype **a** x α fusion (Hull et al. 2005). This finding supports a role of Sxi1α in inhibiting **a** x α
305 fusion, but the differing properties of Sxi2**a** across experiments remains unclear. A possible explanation
306 could be that a of background α x α fusion in XL280 might influence **a** x α fusion frequency, reducing the
307 detectable difference between wildtype and mutant strains.

308 The AlphaFold3-predicted heterodimer structure of Sxi1α and Sxi2**a** closely resembles the yeast
309 MAT**a**1-MATα2 complex (Li 1998) and the predicted *U. maydis* bW-bE heterodimer, consistent with prior
310 studies (Hull et al. 2002; Hull et al. 2005). This supports the importance of the Sxi1α-Sxi2**a** complex in **a** x
311 α mating. Additionally, lower-confidence predictions suggest that Sxi1α and Sxi2**a** may form homodimers,
312 indicating potential independent roles before cell-cell fusion.
313 In the absence of Sxi1α and/or Sxi2**a**, **a** x α mating is severely impaired, as indicated by the
314 absence of normal hyphae during **a** x α sexual reproduction in the *C. neoformans* reference strain H99
315 and the C. *deneoformans* strains JEC43 and JEC34 (Hull et al. 2002; Hull et al. 2005). However, in our
316 study, we found that the disruption of Sxi1α or Sxi2**a** does not affect the mating morphology and
317 sporulation of the strain XL280 during unisexual reproduction, suggesting that these factors may play
318 distinct roles in α x α versus **a** x α reproduction. The inhibitory role of Sxi1α we identified in cell-cell fusion
319 is unexpected, partly because previous studies concluded that Sxi1α functions post-cell fusion (Hull et al.
320 2002; Hull et al. 2005). Because Sxi1α inhibits cell-cell fusion, it may reduce the efficiency of α cells
321 participating in sexual reproduction. Given the predominance of *MAT*α isolates in natural populations,
322 Sxi1α and Sxi2**a** likely have additional roles beyond **a** x α mating. Over evolutionary time, this reduced
323 mating potential could contribute to the widespread dominance of *MAT*α strains by selecting alternative
324 reproductive strategies or favoring unisexual reproduction. Interestingly, by analyzing the 341 *MATα*
325 clinical and environmental isolates in the *C. neoformans* Strain Diversity Collection (Desjardins et al.
326 2017) through a similar pipeline as reported in our previous work (Huang et al. 2024; Martínez and
327 Magwene), we found there were only two closely related environmental isolates (Muc504-1 and Muc489-
328 1) that harbored an identical high-impact mutation with the *SXI1*α gene, suggesting a highly conserved
329 nature and potential functional importance of *SXI1*α that is yet to be characterized. Further studies are
330 needed to clarify the downstream regulators involved in this novel repression role of Sxi1α.
331 In *S. cerevisiae*, the *MAT*α2 transcription factor functions both as a homodimer and heterodimer
332 with *MAT***a**1, playing key roles in mating-type regulation (Keleher et al. 1988; Herskowitz 1989; Goutte
333 and Johnson 1993). The transcriptional regulation of **a**-specific and haploid-specific genes involves
334 interactions with the transcription factor Mcm1 (Keleher et al. 1988; Elble and Tye 1991). Given this
335 precedent, a similar dual functionality with/without mating partner may exist for the sex-specific HD

336 transcription factor Sxi1α in *Cryptococcus*. Our results suggest that Sxi1α might act as both a positive
337 (e.g., in **a** x α mating development) and a negative regulator (e.g., in α x α cell fusion), potentially
338 explaining why our previous result showed that its deletion does not produce a clear phenotype beyond **a**
339 x α crosses (Hull et al. 2004). This phenomenon is reminiscent of the mitogen-activated protein kinase
340 Kss1 in *S. cerevisiae*, which regulates pseudohyphal differentiation through complex signaling
341 mechanisms and functions as a multifunctional regulator in fungal development with counter-balanced
342 positive and negative roles (Madhani et al. 1997).
343 Taken together, while the HD proteins Sxi1α and Sxi2**a** are dispensable for colony morphology,
344 sporulation, and cell viability during unisexual reproduction, Sxi1α plays a key inhibitory role in both α x α
345 and **a** x α cell fusion, whereas Sxi2**a**'s contributions to this process is unclear. These findings suggest that
346 Sxi1α may have yet to be characterized novel functions during *Cryptococcus* mating that echo those in
347 other well studied fungal species, highlighting the regulatory complexity of sexual reproduction in this
348 important human fungal pathogen.

Data availability

Raw WGS sequencing reads have been deposited in Bioproject: PRJNA1219566.

Acknowledgments

We thank Anna Floyd-Averette for constant support, Connor Larmore and Anna Lehmann for critical reading, Dr. Marco Dias Coelho for suggestions on data presentation, Moayad Shehadeh and Dr. Bian Zhuyun for technical support, and all the members of the Heitman Lab for constructive suggestions. We also thank Dr. Xiaorong Lin (University of Georgia) for sharing the XL280 strains, Dr. Ruiyun Zeng (North Carolina State University) for assistance in data visualization, and Dr. Devi Swain Lenz (Duke's Sequencing and Genomic Technologies Core Facility) for advice and expertise.

Funding

This study was supported by NIH/NIAID R01 grants AI039115-27, AI050113-20, and AI133654-07. J. Heitman is co-director and fellow of the Canadian Institute for Advanced Research (CIFAR) program Fungal Kingdom: Threats & Opportunities.

Conflict of Interest

The authors declare no conflicts of interest.

Literature cited

Abramson J, Adler J, Dunger J, Evans R, Green T, Pritzel A, Ronneberger O, Willmore L, Ballard AJ, Bambrick J, et al. 2024. Accurate structure prediction of biomolecular interactions with AlphaFold 3. Nature. 630(8016):493–500. doi:10.1038/s41586-024-07487-w.

Bian Z, Xu Z, Peer A, Choi Y, Priest SJ, Akritidou K, Dasgupta A, Dahlmann TA, Kück U, Nowrousian M, et al. 2024. Essential genes encoded by the mating-type locus of the human fungal pathogen *Cryptococcus neoformans*. doi:10.1101/2024.12.02.626420. [accessed 2025 Feb 4]. http://biorxiv.org/lookup/doi/10.1101/2024.12.02.626420.

Desjardins CA, Giamberardino C, Sykes SM, Yu C-H, Tenor JL, Chen Y, Yang T, Jones AM, Sun S, Haverkamp MR, et al. 2017. Population genomics and the evolution of virulence in the fungal pathogen *Cryptococcus neoformans*. Genome Res. 27(7):1207–1219. doi:10.1101/gr.218727.116.

380 Dranginis AM. 1990. Binding of yeast al and α2 as a heterodimer to the operator DNA of a haploid-
381 specific gene. Nature. 347(6294):682–685. doi:10.1038/347682a0.

382 Ekena JL, Stanton BC, Schiebe-Owens JA, Hull CM. 2008. Sexual development in *Cryptococcus*
383 *neoformans* requires *CLP1* , a target of the homeodomain transcription factors Sxi1α and Sxi2**a**.
384 Eukaryot Cell. 7(1):49–57. doi:10.1128/EC.00377-07.

385 Elble R, Tye BK. 1991. Both activation and repression of a-mating-type-specific genes in yeast require
386 transcription factor Mcm1. Proc Natl Acad Sci USA. 88(23):10966–10970.
387 doi:10.1073/pnas.88.23.10966.

388 Fan Y, Lin X. 2018. Multiple applications of a transient CRISPR-Cas9 coupled with electroporation
389 (TRACE) system in the *Cryptococcus neoformans* species complex. Genetics. 208(4):1357–
390 1372. doi:10.1534/genetics.117.300656.

391 Fu C, Davy A, Holmes S, Sun S, Yadav V, Gusa A, Coelho MA, Heitman J. 2021. Dynamic genome
392 plasticity during unisexual reproduction in the human fungal pathogen *Cryptococcus*
393 *deneoformans*. Copenhaver GP, editor. PLoS Genet. 17(11):e1009935.
394 doi:10.1371/journal.pgen.1009935.

395 Gillissen B, Bergemann J, Sandmann C, Schroeer B, Bölker M, Kahmann R. 1992. A two-component
396 regulatory system for self/non-self recognition in *Ustilago maydis*. Cell. 68(4):647–657.
397 doi:10.1016/0092-8674(92)90141-X.

398 Goutte C, Johnson AD. 1988. a1 Protein alters the dna binding specificity of α2 repressor. Cell.
399 52(6):875–882. doi:10.1016/0092-8674(88)90429-1.

400 Goutte C, Johnson AD. 1993. Yeast a1 and α2 homeodomain proteins form a DNA-binding activity with
401 properties distinct from those of either protein. Journal of Molecular Biology. 233(3):359–371.
402 doi:10.1006/jmbi.1993.1517.

403 Heimel K, Scherer M, Schuler D, Kämper J. 2010. The *Ustilago maydis* Clp1 protein orchestrates
404 pheromone and *b* -dependent signaling pathways to coordinate the cell cycle and pathogenic
405 development. The Plant Cell. 22(8):2908–2922. doi:10.1105/tpc.110.076265.

406 Herskowitz I. 1989. A regulatory hierarchy for cell specialization in yeast. Nature. 342(6251):749–757.
407 doi:10.1038/342749a0.

408 Hsueh Y-P, Xue C, Heitman J. 2009. A constitutively active GPCR governs morphogenic transitions in
409 *Cryptococcus neoformans*. EMBO J. 28(9):1220–1233. doi:10.1038/emboj.2009.68.

410 Huang J, Larmore CJ, Priest SJ, Xu Z, Dietrich FS, Yadav V, Magwene PM, Sun S, Heitman J. 2024.
411 Distinct evolutionary trajectories following loss of RNA interference in *Cryptococcus neoformans*.
412 Proc Natl Acad Sci USA. 121(47):e2416656121. doi:10.1073/pnas.2416656121.

413 Huang J, Rowe D, Subedi P, Zhang W, Suelter T, Valent B, Cook DE. 2022. CRISPR-Cas12a induced
414 DNA double-strand breaks are repaired by multiple pathways with different mutation profiles in
415 *Magnaporthe oryzae*. Nat Commun. 13(1):7168. doi:10.1038/s41467-022-34736-1.

416 Huang MY, Joshi MB, Boucher MJ, Lee S, Loza LC, Gaylord EA, Doering TL, Madhani HD. 2022. Short
417 homology-directed repair using optimized Cas9 in the pathogen *Cryptococcus neoformans*
418 enables rapid gene deletion and tagging. Rando O, editor. Genetics. 220(1):iyab180.
419 doi:10.1093/genetics/iyab180.

Hull CM, Boily M-J, Heitman J. 2005. Sex-Specific homeodomain proteins Sxi1α and Sxi2 **a** coordinately regulate sexual development in *Cryptococcus neoformans*. Eukaryot Cell. 4(3):526–535. doi:10.1128/EC.4.3.526-535.2005.

Hull CM, Cox GM, Heitman J. 2004. The α-specific cell identity factor Sxi1α is not required for virulence of *Cryptococcus neoformans*. Infect Immun. 72(6):3643–3645. doi:10.1128/IAI.72.6.3643-3645.2004.

Hull CM, Davidson RC, Heitman J. 2002. Cell identity and sexual development in *Cryptococcus neoformans* are controlled by the mating-type-specific homeodomain protein Sxi1α. Genes Dev. 16(23):3046–3060. doi:10.1101/gad.1041402.

Kämper J, Reichmann M, Romeis T, Bölker M, Kahmann R. 1995. Multiallelic recognition: Nonself-dependent dimerization of the bE and bW homeodomain proteins in *Ustilago maydis*. Cell. 81(1):73–83. doi:10.1016/0092-8674(95)90372-0.

Keleher CA, Goutte C, Johnson AD. 1988. The yeast cell-type-specific repressor α2 acts cooperatively with a non-cell-type-specific protein. Cell. 53(6):927–936. doi:10.1016/S0092-8674(88)90449-7.

Kües U, Göttgens B, Stratmann R, Richardson WV, O'Shea SF, Casselton LA. 1994. A chimeric homeodomain protein causes self-compatibility and constitutive sexual development in the mushroom Coprinus cinereus. EMBO J. 13(17):4054–4059. doi:10.1002/j.1460-2075.1994.tb06722.x.

Kwon-Chung KJ, Bennett JE. 1978. Distribution of alpha and alpha mating types of *Cryptococcus neoformans* among natural and clinical isolates. American Journal of Epidemiology. 108(4):337–340. doi:10.1093/oxfordjournals.aje.a112628.

Li H, Durbin R. 2009. Fast and accurate short read alignment with Burrows–Wheeler transform. Bioinformatics. 25(14):1754–1760. doi:10.1093/bioinformatics/btp324.

Li T. 1998. Crystal structure of the MATa1/MATalpha2 homeodomain heterodimer in complex with DNA containing an A-tract. Nucleic Acids Research. 26(24):5707–5718. doi:10.1093/nar/26.24.5707.

Li T, Stark MR, Johnson AD, Wolberger C. 1995. Crystal structure of the MATa1/MATα2 homeodomain heterodimer bound to DNA. Science. 270(5234):262–269. doi:10.1126/science.270.5234.262.

Lin X, Hull CM, Heitman J. 2005. Sexual reproduction between partners of the same mating type in *Cryptococcus neoformans*. Nature. 434(7036):1017–1021. doi:10.1038/nature03448.

Madhani HD, Styles CA, Fink GR. 1997. MAP kinases with distinct Inhibitory functions impart signaling specificity during yeast differentiation. Cell. 91(5):673–684. doi:10.1016/S0092-8674(00)80454-7.

Martínez CZ, Magwene PM. FungalPop: A biofinformatics pipeline for building population genomic databases for fungal organisms. in prep Funded by NIH R01AI133654.

Mead ME, Stanton BC, Kruzel EK, Hull CM. 2015. Targets of the Sex Inducer homeodomain proteins are required for fungal development and virulence in *Cryptococcus neoformans*. Mol Microbiol. 95(5):804–818. doi:10.1111/mmi.12898.

Meng EC, Goddard TD, Pettersen EF, Couch GS, Pearson ZJ, Morris JH, Ferrin TE. 2023. UCSF ChimeraX : Tools for structure building and analysis. Protein Science. 32(11):e4792. doi:10.1002/pro.4792.

459 Phadke SS, Feretzaki M, Heitman J. 2013. Unisexual reproduction enhances fungal competitiveness
460 bypromoting habitat exploration via hyphal growth and sporulation. Eukaryot Cell. 12(8):1155–
461 1159. doi:10.1128/EC.00147-13.

462 Roth C, Sun S, Billmyre RB, Heitman J, Magwene PM. 2018. A high-resolution map of meiotic
463 recombination in *Cryptococcus deneoformans* demonstrates decreased recombination in
464 unisexual reproduction. Genetics. 209(2):567–578. doi:10.1534/genetics.118.300996.

465 Sun S, Billmyre RB, Mieczkowski PA, Heitman J. 2014. Unisexual reproduction drives meiotic
466 recombination and phenotypic and karyotypic plasticity in *Cryptococcus neoformans*. Butler G,
467 editor. PLoS Genet. 10(12):e1004849. doi:10.1371/journal.pgen.1004849.

468 Sun S, Coelho MA, David-Palma M, Priest SJ, Heitman J. 2019. The evolution of sexual reproduction and
469 the mating-type Locus: links to pathogenesis of *Cryptococcus* human pathogenic fungi. Annu Rev
470 Genet. 53(1):417–444. doi:10.1146/annurev-genet-120116-024755.

471 Sun S, Fu C, Ianiri G, Heitman J. 2020. The pheromone and pheromone receptor mating-type locus is
472 involved in controlling uniparental mitochondrial inheritance in *Cryptococcus*. Genetics.
473 214(3):703–717. doi:10.1534/genetics.119.302824.

474 Sun S, Priest SJ, Heitman J. 2019. *Cryptococcus neoformans* mating and genetic Crosses. Current
475 Protocols in Microbiology. 53(1):e75. doi:10.1002/cpmc.75.

476 Vollmeister E, Schipper K, Baumann S, Haag C, Pohlmann T, Stock J, Feldbrügge M. 2012. Fungal
477 development of the plant pathogen *Ustilago maydis*. FEMS Microbiol Rev. 36(1):59–77.
478 doi:10.1111/j.1574-6976.2011.00296.x.

479 Wahl R, Zahiri A, KÃ¤mper J. 2010. The *Ustilago maydis b* mating type locus controls hyphal proliferation
480 and expression of secreted virulence factors *in planta*. Molecular Microbiology. 75(1):208–220.
481 doi:10.1111/j.1365-2958.2009.06984.x.

482 Xue C, Tada Y, Dong X, Heitman J. 2007. The human fungal pathogen *Cryptococcus* can complete its
483 sexual cycle during a pathogenic association with plants. Cell Host & Microbe. 1(4):263–273.
484 doi:10.1016/j.chom.2007.05.005.

485 Yadav V, Sun S, Heitman J. 2023. On the evolution of variation in sexual reproduction through the prism
486 of eukaryotic microbes. Proc Natl Acad Sci USA. 120(10):e2219120120.
487 doi:10.1073/pnas.2219120120.

488 Yan Z, Hull CM, Heitman J, Sun S, Xu J. 2004. SXI1α controls uniparental mitochondrial inheritance in
489 *Cryptococcus neoformans*. Current Biology. 14(18):R743–R744. doi:10.1016/j.cub.2004.09.008.

490 Zhai B, Zhu P, Foyle D, Upadhyay S, Idnurm A, Lin X. 2013. Congenic strains of the filamentous form of
491 *Cryptococcus neoformans* for studies of fungal morphogenesis and virulence. Infect Immun.
492 81(7):2626–2637. doi:10.1128/IAI.00259-13.

493

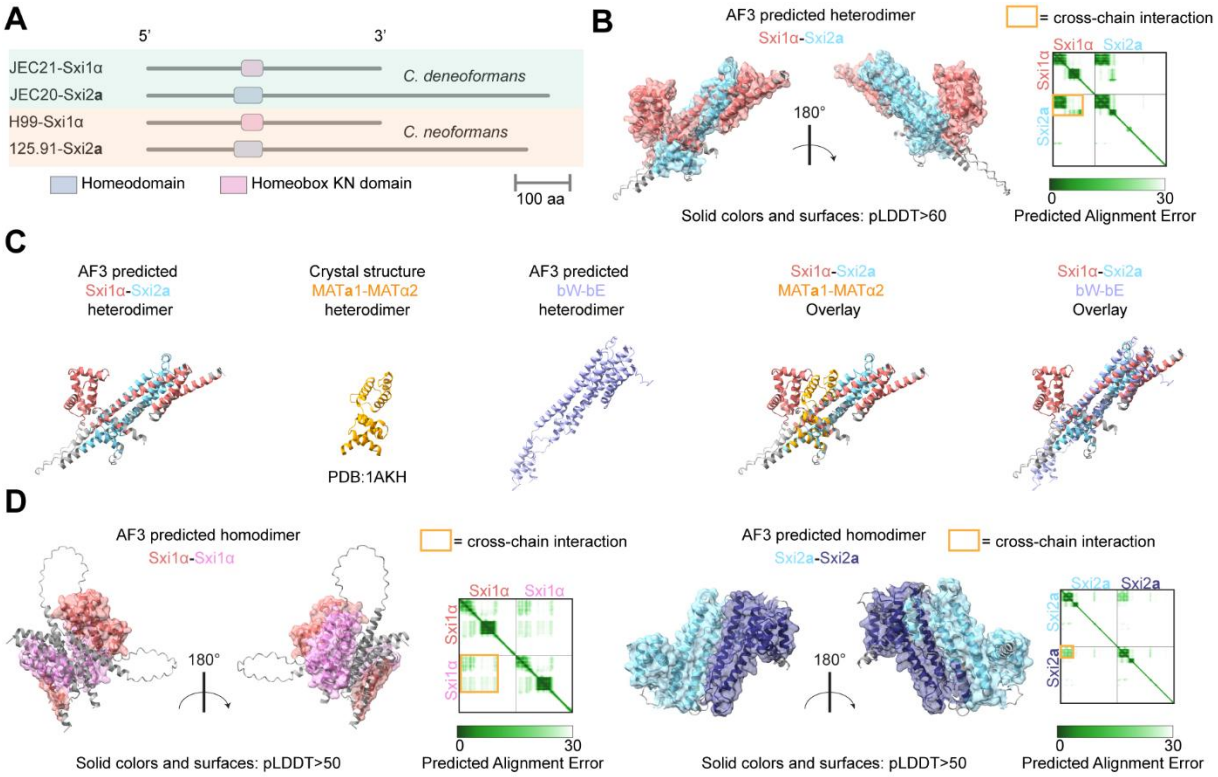

Figure 1. AlphaFold3 predicted heterodimer and homodimers of Sxi1α and Sxi2a.

(A) Predicted domain structures of Sxi1α and Sxi2**a** in *C. neoformans* and *C. deneoformans*. (B) AlphaFold3 (AF3)-predicted heterodimer structure of Sxi1α and Sxi2**a** from *C. deneoformans* JEC21 and JEC20. C-terminal disordered regions were hidden for visualization. Only regions with a predicted local distance difference test (pLDDT) score >60 were colored and surfaced. The predicted alignment error (PAE) plot of the predicted Sxi1α-Sxi2**a** heterodimer is displayed in the right panel. (C) Overlay of AlphaFold3-predicted Sxi1α-Sxi2**a** heterodimer with crystal structure of MAT**a**1-MATα2 (from *S. cerevisiae*, PDB:1AKH) and predicted bW-bE heterodimer (from *U. maydis*, with high confidence ipTM = 0.74 pTM = 0.64). Pairing was performed with the “Matchmaker” function in Chimera X. (D) AlphaFold3-predicted homodimer structures with PAE plots for Sxi1α-Sxi1α (left panel) and Sxi2**a**-Sxi2**a** (right panel). Only regions with a pLDDT score >50 were colored and surfaced.

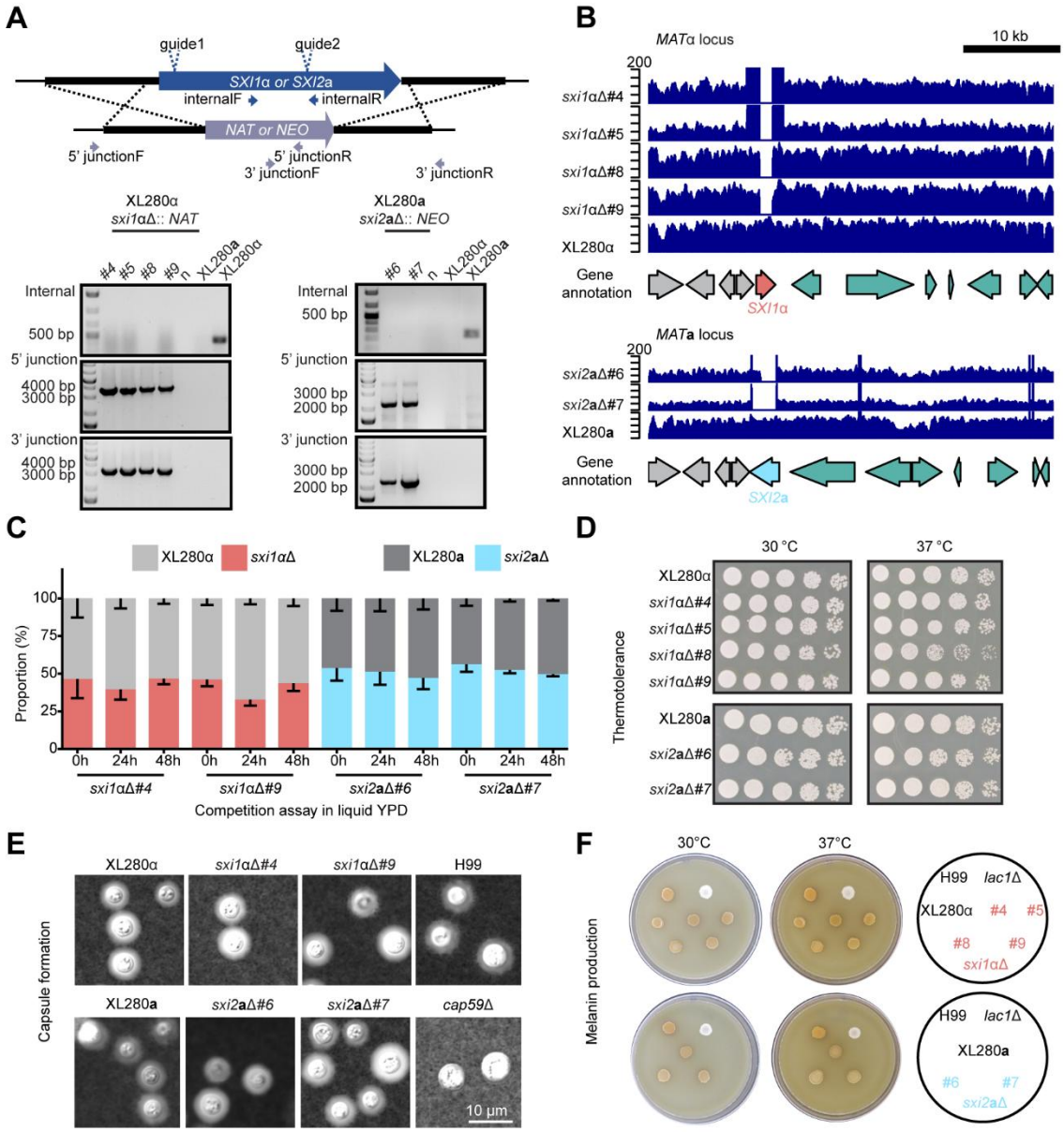

Figure 2. Sxi1α and Sxi2a are not involved in growth, capsule formation and melanin production. (A) Generation of *sxi1*α*Δ* and *sxi2***a***Δ* mutants in XL280α and XL280**a**, respectively. Transformants were verified through internal PCR targeting the ORF, along with 5' and 3' junction PCRs specific to the drug resistance marker to confirm proper integration at the genomic locus. (B) Whole-genome sequencing (WGS) reads mapping confirming the complete or partial deletion of *SXI1*α and *SXI2***a**. Genes located outside or inside the mating-type locus are labeled gray and green, respectively, with *SXI1*α labeled red and *SXI2***a** blue. (C) *In vitro* competition assays between *sxi1*α*Δ* and *sxi2***a***Δ* mutants, each carrying either the *NAT* or *NEO* resistance markers, and the corresponding XL280 wildtype strains. The assay was

517 performed in liquid YPD with four independent replicates after 0, 24, and 48 h of incubation. Error bars
518 indicate standard deviation. (D) Serial dilutions of *sxi1*α**Δ** and *sxi2***a**Δ mutants, along with the
519 corresponding XL280 wildtype strains, were spotted on solid YPD media and incubated at 30°C and
520 37°C. (E) Saturated cultures of the indicated strains, grown in RPMI medium, were stained with India ink
521 to visualize capsule formation. The H99 strain and isogenic *cap59*Δ mutant served as positive and
522 negative controls, respectively. (F) Overnight cultures of the indicated strains were spotted on Niger seed
523 medium to monitor melanin formation. The H99 strain and isogenic *lac1*Δ mutant served as positive and
524 negative controls, respectively.

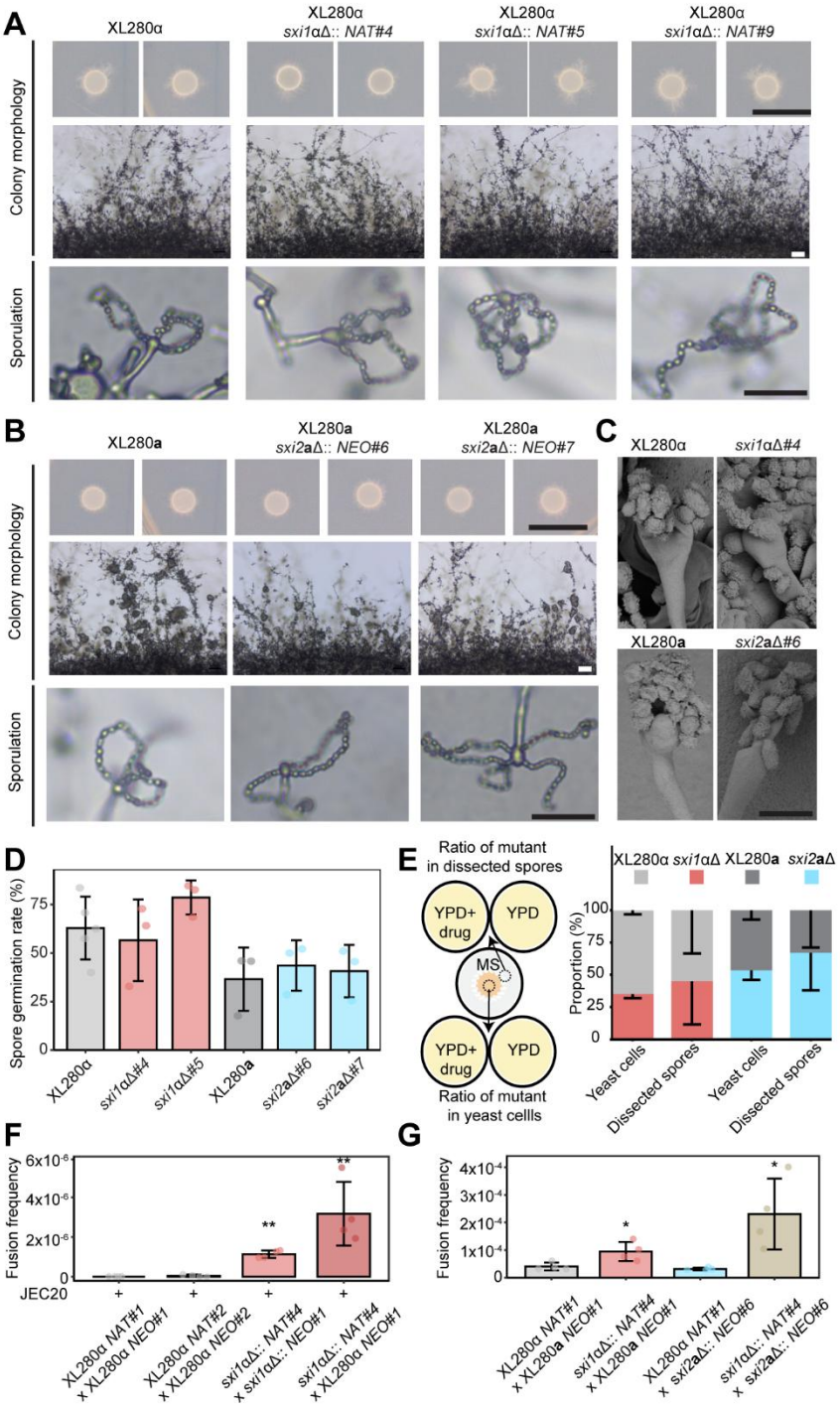

Figure 3. Sxi1α and Sxi2a are not required for hyphal growth or basidium and spore production but are important for cell-cell fusion.

(A and B) Colony morphology, self-filamentation, and sporulation phenotypes of independent *sxi1*αΔ (A) and *sxi2***a**Δ (B) mutants on MS media. Scale bars, 1 cm (upper panel), 100 μm (middle panel) and 20 μm (bottom panel). (C) Scanning electron microscopy (SEM) analysis of basidia and basidiospores from the

531 indicated solo-culture on MS media. Samples were grown on MS media for 1 to 2 weeks before
532 microscopy. Scale bar: 5 μm. (D) Germination rate of random spores dissected from the indicated solo-
533 cultures. At least 3 replicates were performed for each strain (indicated by dots). The height of the bar
534 indicates the mean and error bars depict the standard deviation among the replicates. (E) Competition
535 assays between *sxi1*αΔ, *sxi2***a**Δ mutants, each carrying either the *NAT* or *NEO* resistance marker, and the
536 corresponding XL280 wildtype strain. The assay was performed on MS medium. Spores at the periphery
537 were dissected and transferred to drug plates to measure the presence of the mutants. Internal yeast
538 cells were counted for normalization. Five different spots were analyzed for each competition. (F)
539 Frequency of α x α fusion for the indicated mating with the assistance of JEC20. Cells from the indicated
540 mating assay on V8 agar (pH = 7.0) for 72 h were plated on YPD + NAT + G418 and YPD to determine
541 the ratio of cell-cell fusion products in the population. ** indicates p-value < 0.01 by using an unpaired
542 student t-test. (G) Frequency of **a** x α fusion for the indicated crosses. Cells from the indicated mating
543 assays on V8 agar (pH=7.0) for 48 h were plated on YPD+NAT+G418 and YPD to determine the ratio of
544 cell-cell fusion products in the population. * Indicates p-value < 0.05 by using an unpaired student t-test.
545